Published in final edited form as:
Mol Biosyst. 2010 February ; 6(2): 349–356. doi:10.1039/b918106g.

Functional characterization of *tlmH* in *Streptoalloteichus hindustanus* E465-94 ATCC 31158 unveiling new insight into tallysomycin biosynthesis and affording a novel bleomycin analog

Meifeng Tao[†,a], **Liyan Wang**[†,a], **Evelyn Wendt-Pienkowski**[a], **Ningning Zhang**[b], **Dong Yang**[b], **Ute Galm**[a], **Jane M. Coughlin**[c], **Zhinan Xu**[*,b], and **Ben Shen**[*,a,c,d]

[a]Division of Pharmaceutical Sciences, University of Wisconsin-Madison, Madison, WI 53705-2222, U.S.A

[b]Institute of Bioengineering, Department of Chemical Engineering and Bioengineering, Zhejiang University, Hangzhou 310027, Zhejiang, China

[c]Department of Chemistry, University of Wisconsin-Madison, Madison, WI 53705-2222, U.S.A

[d]University of Wisconsin National Cooperative Drug Discovery Group, University of Wisconsin-Madison, Madison, WI 53705-2222, U.S.A

Abstract

Tallysomycins (TLMs) belong to the bleomycin (BLM) family of anticancer antibiotics and differ from the BLMs principally by the presence of a 4-amino-4,6-dideoxy-L-talose attached to C-41 of the TLM backbone as part of a glycosylcarbinolamide. To facilitate an understanding of the differences in anticancer activities observed between TLMs and BLMs, we thought to generate des-talose TLM analogs by engineering TLM biosynthesis in Streptoalloteichus hindustanus E465-94 ATCC 31158. Here we report (i) the engineering of the *ΔtlmH* mutant SB8005 strain that produces the two TLM analogs, TLM H-1 and TLM H-2, (ii) production, isolation, and structural elucidation of TLM H-1 and TLM H-2 by NMR and mass spectroscopic analyses as the desired des-talose TLM analogs, and (iii) comparison of the DNA cleavage activities of TLM H-1 with selected TLMs and BLMs. These findings support the previous functional assignment of *tlmH* to encode an α-ketoglutarate-dependent hydroxylase and unveil the TlmH-catalyzed hydroxylation at both C41 and C42 and the TlmK-catalyzed glycosylation of a labile carbinolamide intermediate as the final two steps for TLM biosynthesis. TlmH is apparently distinct from other enzymes known to catalyze carbinolamide formation. The availability of TLM H-1 now sets the stage to study the TlmH enzymology in vitro and to elucidate the exact contribution of the L-talose to the anticancer activities of TLMs in vivo.

Introduction

The tallysomycins (TLMs) belong to the bleomycin (BLM) family of glycopeptide anticancer antibiotics (Fig. 1). [1] The BLMs are currently used clinically, under the trade name Blenoxane®, in combination with a number of other agents for the treatment of a range of lymphomas, skin carcinomas, and head, neck, and testicular cancers. Early

Tel/Fax: 571-87951220, znxu@zju.edu.cn and Tel: 608-263-2673, FAX: 608-262-5245 bshen@pharmacy.wisc.edu.
[†]These authors contributed equally to this work

development of drug resistance and cumulative dose-dependant pulmonary toxicity are the major limitations of BLMs in chemotherapy.[2–4] The development of active and particularly less toxic analogs of this family of anticancer drugs therefore has been intensively pursued in the past three decades.

The BLMs are thought to exert their biological effects through metal-dependent oxidative cleavage of DNA and RNA in the presence of molecular oxygen. The BLMs can be dissected into three functional domains: (i) the N-terminal metal-chelating domain, including the pyrimidoblamic acid and the glycosylated β-hydroxyhistidine moieties, which is responsible for binding of the transition metal and oxygen activation, (ii) the C-terminal domain, including the threonine, bithiazole and terminal amine moieties, which is responsible for DNA binding, and (iii) a linker domain, (2*S*, 3*S*, 4*R*)-4-amino-3-hydroxy-2-methylvaleric acid (AHM), which is essential for efficient sequence-selective DNA cleavage by the BLMs (Fig. 1).[2–4] The sugar moiety is known to enhance DNA cleavage efficacy. The recently reported crystal structure of a DNA-bound Co (III)-BLM B2 complex suggested that the disaccharide enhances the binding of BLMs to DNA via intermolecular hydrogen bonding, thereby allowing the metal binding domain to adopt an optimized position relative to the target cleavage site.[5]

The mechanism by which TLMs generate DNA strand breaks appears to be similar to that envisioned for the BLMs, i.e., complex formation with a transition metal and oxygen followed by free radical formation.[6–8] TLM S10b, a TLM analog obtained by fermenting the producing strain in a medium supplemented with 1,4-diaminobutane, exhibited antitumor activity similar to that of the BLMs but with less severe toxicity in preclinical studies. However, TLM S10b failed to yield the desired response in phase II clinical trials.[9–11] Since one of the principal structural differences between the BLMs and the TLMs is the extra talose sugar attached to the aminoethylbithiazole moiety of the TLM backbone (Fig. 1), we sought to generate des-talose TLM analogs to facilitate an understanding of the differences in anticancer activities observed between the TLMs and the BLMs.

Previously, we have cloned and characterized the biosynthetic gene clusters for three members of the BLM family – the BLMs from *Streptomyces verticillus* ATCC 15003,[12–14] the TLMs from *Streptoalloteichus hindustanus* E465-94 ATCC 31158,[1] and zorbamycin from *Streptomyces flavoviridis* ATCC 21892[15] – and established a unified pathway for their biosynthesis. Close examination of the gene clusters encoding TLM and BLM biosynthesis revealed that, while both clusters contain the genes encoding the synthesis and attachment of the L-gulose-3-*O*-carbamoyl-D-mannose disaccharide, the *tlm* gene cluster contains a small operon, consisting of three genes, *tlmHJK*, the counterpart of which is absent from the *blm* cluster.[1,12] This operon has been proposed to be involved in biosynthesis of the 4-amino-4,6-dideoxy-L-talose and its attachment to the TLM hybrid polyketide-peptide backbone as part of a glycosylcarbinolamide.[16]

Recently, we have characterized TlmK as a glycosyltransferase that catalyzes the attachment of the talose sugar to the aminoethylbithiazole moiety of TLM, thereby stabilizing a labile carbinolamide intermediate in the TLM biosynthetic pathway.[16] Here we now report (i) the inactivation of *tlmH* in *S. hindustanus* to abolish TLM A and TLM B production, (ii) isolation and structural characterization of two des-talose TLM analogs, TLM H-1 and TLM H-2, from the *ΔtlmH* mutant, and (iii) comparison of the DNA cleavage activities of TLM H-1 with selected TLMs and BLMs. These findings support the previous functional assignment of *tlmH* to encode an α-ketoglutarate-dependent hydroxylase, unveil new insight into TLM biosynthesis, and set the stage to dissect the role the talose moiety may play in TLM's DNA cleavage, pulmonary toxicity, and anticancer activities.

Results

In-frame Deletion of *tlmH* in *S. hindustanus*

Inactivation of the *tlmH* gene in *S. hindustanus* afforded the *ΔtlmH* mutant SB8005 strain that abolished TLM A and TLM B production and instead accumulated two new intermediates, TLM H-1 and TLM H-2. The *ΔtlmH* mutant SB8005 strain was constructed from the *S. hindustanus* wild-type strain by following the λRED-mediated, PCR-targeting mutagenesis method (Fig. 2A). [17] The plasmid pBS8016 that harbors an in-frame deletion of the *tlmH* allele was introduced into *S. hindustanus* by electroporation followed by screening for double crossover homologous recombination. Six desired mutants (SB8005) were isolated whose predicted genotypes were confirmed by Southern hybridization (Fig. 2B). Fermentation of SB8005, with the *S. hindustanus* wild-type strain as a positive control, followed by HPLC analysis of metabolite produced showed that (i) production of TLM A and TLM B was completely abolished in SB8005 and (ii) instead, SB8005 produced two new metabolites, with retention times of 14.5 min (TLM H-1) and 16.2 min (TLM H-2), respectively (Fig. 2C). SB8005 produced TLM H-1 with an estimated titer of ~8 mg/L under the original fermentation conditions, and TLM H-1 titer can be improved up to 175 mg/L in the optimized production medium.

Isolation and Structural elucidation of the new Metabolites accumulated by the *ΔtlmH* Mutant SB8005 Strain

Isolation of the two new metabolites produced by SB8005 was carried out by multiple steps of chromatography as described previously for TLM A, TLM B, and other TLM analogs. The structure of TLM H-1 was elucidated by a combination of MS and ^{1}H and ^{13}C NMR spectroscopic analyses as well as by comparison to the ^{1}H and ^{13}C NMR data in the literature on the TLMs and BLMs, in particular to those of TLM A and BLM A2.[1,18] Upon ESI-MS analysis, the purified TLM H-1-Cu complex yielded a molecular ion at *m/z* of 808.3, consistent with the $[TLM\ H\text{-}1 + Cu]^{2+}$ ion (calculated 1616.6). The high resolution MALDI-FTMS of Cu-free TLM H-1 afforded a molecular ion at *m/z* of 1554.6756, which corresponded to the $[TLM\ H\text{-}1 + H]^{+}$ ion with the molecular formula $C_{62}H_{99}N_{21}O_{22}S_2{+}H^{+}$ (calculated 1554.6788). The ^{1}H and ^{13}C NMR spectra of TLM H-1 are very similar to those of TLM A except that (i) the signals of the talose sugar were absent, (ii) the signals for the two oxygen bearing methine carbons, C-41 (δ 83.4) and C-42 (δ 74.0), disappeared, and (iii) two methylene carbons at δ 41.8 and δ 34.8 were detected instead. Comparison of the NMR data of TLM H-1 with those of BLM A2 indicated that, with the exception of the aberrant signals resulting from varying terminal amine moieties, there were only two apparent differences: (i) TLM H-1 lacked the C-35 methyl group of BLM A2 (δ_H 1.10, δ_C 15.1) and (ii) the methine signals of C-34 (δ_H 2.45, δ_C 45.8) in BLM A2 were replaced by a new methylene signal at [δ_H 2.44 (15.0, 3.0), 2.50 dd (15.0, 9.5); δ_C 42.5] in TLM H-1. Taken together, these data suggested that TLM H-1 has the same hybrid polyketide-peptide backbone as TLM A but lacks the talose sugar moiety and the two hydroxyl groups at C-41 and C-42. This deduced structure was further confirmed by detailed analysis of 2D ^{1}H-^{1}H COSY, TOCSY, HSQC, and HMBC data for TLM H-1 (Fig. 3A). The latter analyses also enabled the full ^{1}H and ^{13}C NMR spectroscopic assignments as summarized in Table 1

The *S. hindustanus* wild-type strain produces TLM A and TLM B with TLM A as the predominant metabolite. A similar metabolite profile was also observed for SB8005 upon HPLC analysis with TLM H-1 and TLM H-2 as the major and minor metabolite, respectively (Fig. 2C). Isolation and purification of TLM H-2 was not pursued due to its extremely low titer. However, upon LC-ESI-MS analysis, TLM H-2 afforded a molecular ion at *m/z* of 744.4, indicative of the $[TLM\ H\text{-}2 + Cu]^{2+}$ ion with a molecular weight of 1488.8. This suggests that TLM H-2 differs from TLM H-1 by mass of 128, equivalent to a

β-lysine moiety (Fig. 1). Since TLM A differs from TLM B in its terminal amine with an extra β-lysine residue, TLM H-2, in a structural analogy to TLM B, was deduced to have the same hybrid polyketide-peptide backbone as TLM H-1 but with the terminal amine of TLM B (Fig. 3B).

DNA Cleavage Activity of TLM H1

Removal of the talose sugar from TLM A resulted in only slightly decreased DNA cleavage activity. TLM H-1 was compared to TLM A, BLM A2 and B2 for its ability to cleave pBluescript II SK(+) supercoiled plasmid DNA in the presence of Fe^{2+} as described previously.[14,19] BLM-mediated single-strand cleavage first results in the conversion of supercoiled plasmid DNA (form A) to open-circular plasmid DNA (form B), and double-strand cleavage subsequently generates linearized plasmid DNA (form C). In this assay, TLM A, BLM A2 and B2 showed nearly 100% plasmid relaxation and ~50% plasmid linearization at concentrations of 1 μM each. TLM H-1 was nearly as efficient as TLM A, BLM A2, or BLM B2 in producing double strand breaks, generating equally intense signals for forms B and C. However, even at concentrations of 2 μM TLM H-1 ~20% DNA form A was retained, resulting in a mixture of supercoiled, relaxed, and linearized plasmid DNA (Fig. 4). The observed DNA cleavage activity was concentration dependent for all the compounds tested.

Discussion

Although numerous BLM and TLM analogs have been synthesized,[20–24] total synthesis of these compounds in sufficient quantities for preclinical and clinical studies remains challenging due to the complex scaffold of the BLM family of anticancer antibiotics. Recent cloning and characterization of the BLM, TLM, and zorbamycin biosynthetic gene clusters from *S verticillus* ATCC 15003,[12–14] *S. hindustanus* E465-94 ATCC 31158 (34), and *S. flavoviridis* ATCC 21892[15] have provided significant advancements towards the targeted production of novel BLM and TLM analogs via metabolic pathway engineering approaches. Moreover, in vivo and in vitro characterization of these clusters promises to facilitate detailed investigations of the biosynthetic pathways as well as the functional roles of the structural entities of the BLM family of anticancer antibiotics.[14,16,25–29]

In this study, we focused on specific questions arising from the differences in sugar decoration of the hybrid peptide-polyketide backbone, particularly of the TLMs. The functional role of the carbohydrate moieties of BLM and related analogs has been thought to involve cell recognition, cellular uptake, metal-ion coordination, and/or DNA affinity.[2–5] Therefore it is of special interest to generate new but related analogs differing only in their carbohydrate pattern to closely investigate the influence of the sugar decoration on the activity profiles of those compounds. The manipulation of biosynthetic genes involved in sugar biosynthesis and attachment seemed to be a promising strategy to achieve these goals as exemplified by the recent production of a decarbamoyl-BLM.[14]

The TLMs differ from the BLMs principally by the additional sugar 4-amino-4,6-dideoxy-L-talose as part of a glycosylcarbinolamide (Fig. 1). TLM S10b, a member of the TLMs that exhibited similar activity to that of the BLMs in preclinical studies, however, failed to yield the desired response in phase II clinical trials.[9–11] Cloning and sequencing of the *tlm* cluster from *S. hindustanus* have indeed unveiled three genes, *tlmH*, *tlmJ*, and *tlmK*, encoding an α-ketoglutarate-dependent hydroxylase, aminotransferase, and glycosyltransferase, respectively, that were proposed to be involved in the biosynthesis of the 4-amino-4,6-dideoxy-L-talose and its subsequent attachment to the TLM hybrid polyketide-peptide backbone.[1] In order to generate a TLM analog lacking the L-talose moiety, it seemed logical to inactivate the *tlmK* glycosyltransferase gene and isolate the corresponding des-talose

TLM. The *ΔtlmK* mutant SB8003 strain, however, failed to accumulate the predicted TLM analog, whose carbinolamide moiety apparently undergoes facile hydrolytic fragmentation to afford several degradation products; none of these products showed noticeable DNA cleavage activity.[16] Inspired by these findings, we set out to inactivate the *tlmH* gene for the production of des-talose TLM analogs. The *ΔtlmH* mutant SB8005 strain indeed produced the desired des-talose TLM analog, TLM H-1. Although SB8005 produced TLM H-1 in a moderate titer (~8 mg/L) under the original fermentation conditions, we have now optimized its production medium, thereby increasing the TLM H-1 titer up to 175 mg/L, thus providing a reliable supply of the compound for future mechanistic characterizations and preclinical studies.

Isolation of TLM H-1 from the *ΔtlmH* mutant SB8005 strain supports the previous functional assignment of TlmH as an α-ketoglutarate-dependent hydroxylase,[1] further revealing that TlmH is responsible for hydroxylating both C-41 and C-42 to afford the carbinolamide intermediate. We have previously demonstrated in the characterization of the *ΔtlmK* mutant SB8003 strain that the carbinolamide intermediate requires the ensuing glycosylation to stabilize an intrinsically labile hemiaminal functional group.[16] Taken together, these results establish TlmH and TlmK to catalyze the last two steps for TLM biosynthesis, and the coupling of TlmH and TlmK catalysis underscores once again nature's ingenuity in channeling otherwise unstable intermediates for the biosynthesis of complex natural products (Fig. 5).

The TlmH-catalyzed hydroxylation to afford a carbinolamide is of particular mechanistic interest since only a few enzymatic processes for carbinolamide formation are known. For instance, the C-9 carbinolamide in maytansinoid biosynthesis was found to be catalyzed by the Asm21 carbamoyltransferase in *Actinosynnema pretiosum*.[30] Approximately 50% of all known mammalian peptide hormones possess a C-terminal α-amide function, which has been found to be essential for hormone activity. The formation of these hormones has been shown to be catalyzed by a bifunctional peptidylglycine α-amidating monooxygenase via the oxidation of the glycine extended precursor peptides to a carbinolamide intermediate followed by the catalytic breakdown, in a second active site of the same enzyme, to the α-amidated peptide and glyoxylate.[31] TlmH is apparently distinct from Asm21 or peptidylglycine α-amidating monooxygenase, representing yet another mechanism for carbinolamide formation. TlmH and its substrate TLM H-1 therefore now provide an outstanding opportunity to study this fascinating enzymatic formation of carbinolamide in vitro.

Investigation of TLM H-1 for DNA relaxation and linearization in comparison to TLM A, BLM A2, and BLM B2 indicates a minor role of the L-talose sugar for efficient cleavage activity (Fig. 4). The plasmid linearization efficiency observed for TLM H-1 was very similar to that of the TLM and BLM standards. The plasmid relaxation reaction, however, was not driven to completion by TLM H-1 as opposed to the control reactions with TLM A, BLM A2, and BLM B2. This observation indicates that the L-talose moiety enhances the interaction of the TLMs especially with the DNA double strand resulting in equal cleavage efficiencies of the TLMs and BLMs despite their slightly different linker regions and their different terminal amines (Fig. 1). In depth spectroscopic and mechanistic studies of TLM H-1 in comparison to other TLMs and BLMs will allow elucidation of the exact contribution of the L-talose sugar to DNA binding, cleavage activity, cell-recognition and cell-uptake mechanisms, and the availability of TLM H-1 should greatly facilitate these studies.

Conclusions

TLMs belong to the BLM family of anticancer antibiotics but differ from the BLMs principally by the presence of a 4-amino-4,6-dideoxy-L-talose attached to C-41 of the TLM backbone as part of a glycosylcarbinolamide. Inactivation of *tlmH* in *S. hindustanus* E465-94 ATCC 31158 afforded the *ΔtlmH* mutant SB8005 strain that produces the two TLM analogs, TLM H-1 and TLM H-2. Isolation and structural elucidation of TLM H-1 and TLM H-2 by NMR and mass spectroscopic analyses support the previous functional assignment of *tlmH* to encode an α-ketoglutarate-dependent hydroxylase and unveil the TlmH-catalyzed hydroxylation at both C41 and C42 and the TlmK-catalyzed glycosylation of a labile carbinolamide intermediate as the final two steps for TLM biosynthesis. Comparison of TLM H-1 with selected TLMs and BLMs shows that the removal of the talose sugar from TLM A resulted in only slightly decreased DNA cleavage activity in vitro. The availability of TLM H-1 now sets the stage to study the TlmH enzymology in vitro and to elucidate the exact contribution of the L-talose to the anticancer activities and pulmonary toxicity of TLMs in vivo.

Materials and Methods

Bacterial Strains, Plasmids, and Culture Conditions

The *S. hindustanus* E465-94 ATCC 31158 wild-type strain and the *ΔtlmH* in-frame deletion mutant SB8005 strain generated in this study were cultivated at 30°C on ISP4 medium supplemented with 28 mM $MgCl_2$.[1] *Escherichia coli* DH5α[32] and *E. coli* ET12567[33] were grown at 37°C in liquid or on solid Luria-Bertani medium.[32] *E. coli* BW25113/pIJ790 and *E. coli* BT340 were cultivated according to the protocols provided by the λRED-mediated, PCR-targeting mutagenesis kit.[17] pBS8008,[1] a cosmid carrying the 41.6-kb *S. hindustanus* DNA that covers part of the *tlm* gene cluster including *tlmH*, was used to construct the *ΔtlmH* in-frame deletion construct pBS8016. pBS8010,[16] a plasmid carrying the kanamycin resistance gene flanked by two FRT sites, was used as a template to amplify the FRT-*neo* cassette.

DNA Isolation and Manipulation

DNA isolation and manipulation in *E. coli*[32] and *S. hindustanus*[34] were carried out according to standard procedures. Southern analysis using digoxigenin labeled DNA probes was performed according to the protocol provided by the manufacturer (Roche, Indianapolis, IN). Introduction of cosmid DNA into *S. hindustanus* by electroporation was carried out as previously described.[1]

Construction of the *ΔtlmH* In-frame Deletion Mutant SB8005 Strain

The *ΔtlmH* in-frame deletion mutant was constructed via a homologous recombination strategy following a previously described procedure.[1] First, the FRT-*neo* cassette, amplified from pBS1010 using oligonucleotides tlmH-frt1 (5'-gggaccgcgtcggttcaccagcacgcgccgtcgggaatgtatgATTCCGGGGATCCGTCGACC-3') and tlmH-frt2 (5'-atcatgcccatgccgccgcctccgcgtcgccgcccgcgtcaTGTAGGCTGGAGCTGCTTC-3') (low case letters represent DNA sequence originating from *S. hindustanus*, and upper case letter represent DNA sequence flanking the FRT-*neo* cassette from pBS8010), was used to construct the *ΔtlmH* in-frame mutation in pBS8008 by the λRED-mediated, PCR-targeting mutagenesis method.[17] This replaced the *tlmH* gene in pBS8008 with the FRT-*neo* cassette to afford pBS8015. Next, the FRT-*neo* cassette in pBS8015 was removed by the FLP recombinant function provided by *E. coli* BT340 according to the instructions of the λRED-mediated, PCR-targeting mutagenesis kit.[17] In the resulting cosmid pBS8016, the entire

tlmH gene was deleted, leaving only the ATG start codon, the TGA stop codon, and the 81-bp stretch of unrelated nucleotides between the ATG and TGA codons. Finally, pBS8016, passed through *E. coli* ET12567 to produce unmethylated plasmid DNA, was introduced into the *S. hindustanus* wild-type strain by electroporation.[1] Recombinant strains resulting from the first crossover homologous recombination event were selected by thiostrepton resistance (50 μg/mL).[34] They were then restreaked onto nonselective plates for growth and sporulation to encourage the second crossover homologous recombinant event. The resulting spores were finally plated out and screened for thiostrepton sensitive colonies.

The genotype of the thiostrepton sensitive isolates was first determined by PCR using oligonucleotides tlmH-up and tlmH-down. This resulted in the identification of six *ΔtlmH* inframe deletion mutants named SB8005. The genotype of the SB8005 strains was further confirmed by Southern analysis using a 1.55-kb *tlmH* fragment as a probe. The latter was amplified from the *S. hindustanus* wild-type strain using primers tlmH-up (5'-GGGATCGGGACCGCGTCGG-3') and tlmH-down (5'-GGGTAGCCGCCGTAGTGCAG-3').

Production and Isolation of TLM A, TLM B, TLM H-1, and TLM H-2

Production and isolation of TLM A and TLM B from the *S. hindustanus* wild-type strain and TLM H-1 and TLM H-2 from the *S. hindustanus ΔtlmH* mutant SB8005 strain were carried out as described previously.[1] The original seed medium consisted of 1.5% glucose, 0.2% yeast extract, 0.5% peptone, 0.05% K_2HPO_4, 0.05% $MgSO_4 \cdot 7H_2O$, 0.5% $CaCO_3$, adjusted to pH 7.2 with 1.0 N HCl. The original production medium consisted of 2.5% sucrose, 0.5% glucose, 3% cottonseed meal, 3% distiller's grains and solubles (Sigma-Aldrich, Milwaukee WI.), 0.3% $(NH_4)_2SO_4$, 0.01% $CuSO_4 \cdot 5H_2O$, 0.003% $ZnSO_4.7H_2O$, 0.5% $CaCO_3$, adjusted to pH 7.2 with 1.0 N HCl. Thus, spores of the *S. hindustanus* wild-type or *ΔtlmH* mutant SB8005 strain were inoculated to the seed medium and cultured at 250 rpm, 30°C for 2 days. Five mL of the resultant seed culture was then used to inoculate 50 mL production medium, and incubation continued at 250 rpm, 30°C for 6–8 days.

To isolate TLM A, TLM B, TLM H-1, and TLM H-2 on an analytical scale, the fermentation culture (50 mL) was centrifuged, and the supernatant was collected, adjusted to pH 7.0 with 1.0 M HCl, and mixed with Amberlite® IRC-50 resin (H^+-type, 10 mL). After incubation at room temperature under gentle agitation for 30 min, the resin was packed into a column, washed with 10 bed-volumes of water and drained of excess water. TLM A, TLM B, TLM H-1, and TLM H-2 were eluted off the column with 30 mL of 0.2 M HCl. The eluate was neutralized with 1.0 N NaOH, concentrated to dryness *in vacuo*, and dissolved in 1 mL of H_2O for HPLC analysis.

Analysis and Purification of TLM A, TLM B, TLM H-1, and TLM H-2 by HPLC

Analytical HPLC was carried out on an Apollo C-18 column (5 μ, 250 × 4.6 mm, Alltech Associates, Inc., Deerfield, IL) as described previously.[1] Briefly, the column was equilibrated with 100% solvent A (99.8% H_2O, 0.2% acetic acid) and 0% solvent B (99.8% methanol, 0.2% acetic acid) and developed with a linear gradient (0–5 min, linear gradient from 100% A/0% B to 90% A/10% B; 5–30 min, linear gradient from 90%A/10% B to 0% A/100% B; 30–35 min, 0% A/100% B) at a flow rate of 0.7 mL/min and UV detection at 300 nm using a Varian Prostar 330 PDA detector (Varian, Palo Alto, CA). Under these conditions, TLM A and TLM B from the wild-type strain were eluted with retention times of 11.0 and 12.4 min, while TLM H-1 and TLM H-2 from the *ΔtlmH* mutant SB8005 strain were eluted with retention times of 14.5 and 16.2 min, respectively. The materials isolated at this step were about 80% pure. The combined yields of TLM A and TLM B from the wild-type strain and of TLM H-1 and TLM H-2 from the *ΔtlmH* mutant SB8005 strain was

estimated to be ~18 mg/L and ~8 mg/L, respectively. Due to its low titer, isolation of TLM H-2 was not pursued. TLM H-2 was directly analyzed, as a mixture of TLM H-1 and TLM H-2, by LC-electrospray ionization-mass spectroscopy (ESI-MS), yielding *m/z* at 744.4 for the $[\text{TLM H-2-Cu}]^{2+}$ ion.

To isolate TLM H-1 on a preparative scale, the fermentation culture (10.0 L) was centrifuged, and the supernatant was collected, adjusted to pH 7.0 with 1.0 M HCl, and loaded onto an Amberlite® IRC-50 column (H^+-type, 1.0 L). After washing the column with three bed-volumes of H_2O, the TLM H-1 was eluted with 3 L of 0.2 M HCl. The resulting eluate was loaded onto an Amberlite® XAD-16 column (500 mL). After washing with three bed-volumes of H_2O, TLM H-1 was eluted with 1 L of 80 % methanol. The eluate was concentrated *in vacuo* to 10 mL and loaded to a CM-Sephadex C-25 (50 × 20 mm) column. The column was washed with three bed-volumes of H_2O and subsequently eluted with three bed-volumes of 0.05 M and 1.0 M NH_4OAc, respectively. Fractions containing TLM H-1 were found in the 1.0 M NH_4OAc eluate. These fractions were loaded to an Amberlite® XAD-16 column (50 × 20 mm), washed with three bed-volumes of H_2O, and eluted with three bed-volumes of 80% methanol. The eluate was concentrated *in vacuo* to 2 mL for final purification of TLM H-1 by semipreparative HPLC on an Altima C18 column (250 × 10 mm, Alltech Associates, Inc., Deerfield, IN). HPLC was carried out on the same instrument and with the same detector under the following conditions: the column was equilibrated with 100% solvent A (99.9% H_2O, 0.1% TFA) and 0% solvent B (99.9% methanol, 0.1% TFA) and developed with a linear gradient from 100% A/0% B to 50% A/50% B in 20 min at a flow rate of 3 mL/min and UV detection at 300 nm. The retention time of TLM H-1 under these conditions was 16.5 min. Upon removal of the solvent, TLM H-1 was purified as a blue powder of a TLM H-1-Cu complex (15.0 mg). Cu-free TLM H-1 (11.5 mg) was obtained as a pale white powder by treating the TLM H-1-Cu complex with 0.5 M EDTA-Na (pH 7.3) solution followed by an additional step of HPLC purification under the same conditions as described previously.[1]

MS and NMR Analysis of TLM H-1 and TLM H2

LC-ESI-MS analysis was performed on an Agilent 1100 HPLC-MSD SL quadrupole mass spectrometer (Santa Clara, CA). High resolution Matrix-Assisted Laser Desorption Ionization-Fourier Transform (MALDI-FT) MS analysis was performed on an IonSpec HiResMALDI FT-Mass spectrometer (Lake Forest, CA). NMR data were acquired on a VARIAN Inova-500 (500 MHz) spectrometer (Palo Alto, CA). The sample was dissolved in D_2O with sodium 3-trimethyl silyl [2,2,3,3,-$^2H_4$] propionate as an internal standard.

TLM H-1-Cu complex: light blue powder; ESI-MS *m/z* at 808.3 for the $[\text{TLM H-1-Cu}]^{2+}$ ion. Cu-free TLM H-1: pale white power; $[\alpha]_D$ +36.7 (*c* 0.13, H_2O); UV (H_2O) λ_{max} 228 (ε 23540), 288 (ε 17120) nm; IR (neat) ν_{max} 3400-3200, 1671, 1551, 1435, 1183, 1129 cm^{-1}; ^1H and ^{13}C NMR data, see Table 1; high resolution MALDI-FTMS *m/z* at 1554.6756 for the $[M+H]^+$ ion, $C_{62}H_{99}N_{21}O_{22}S_2 + H^+$ (calculated, 1554.6788).

Medium Optimization of SB8005 for TLM H-1 Production

Individual ingredients in the original production medium were systematically examined to improve TLM H-1 production.[35,36] The final optimized production medium consists of 2% maltose, 3.5% distiller's grains and solubles, 3.5% corn flour, 0.2% $(NH_4)_2SO_4$, 0.005% $CuSO_4 \cdot 5H_2O$, 0.05% $ZnSO_4 \cdot 7H_2O$, 0.4% $CaCO_3$, adjusted to pH 7.2 with 1.0 N NaOH. SB8005 fermented in the optimized production medium at 250 rpm, 30°C for 6–8 days consistently produced TLM H-1 in a titer of ~175 mg/L.

DNA Cleavage Assay

The DNA cleavage assays were performed as described previously.[14,19] Briefly, the assay solution (10 μl), containing ~15 ng of pBluescript SK II(+) plasmid DNA, 10 μM $Fe(NH_4)_2(SO_4)_2 \cdot 6\ H_2O$ (freshly prepared solution in 1 mM H_2SO_4), and the appropriate concentrations of TLM A, TLM H-1, BLM A2, or BLM B2 in 25 mM Tris-HCl buffer, pH 7.5, was incubated at 37°C for 30 min. The reaction was stopped by the addition of 5 mM EDTA and 5 μL of loading dye (30% glycerol containing 0.25% (w/v) bromphenol blue). Samples were applied to a 0.8% agarose gel containing 1 μg/mL ethidium bromide, and gel electrophoresis was carried out in 40 mM Tris-acetate buffer, pH 8.0, containing 1 mM EDTA at 90 V for 1 h. The DNA bands were evaluated under UV light.

Notes and references

1. Tao M, Wang L, Wendt-Pienkowski E, George NP, Galm U, Zhang G, Coughlin JM, Shen B. Mol. BioSyst. 2007; 3:60–74. [PubMed: 17216057]
2. Hecht SM. J. Nat. Prod. 2000; 63:158–168. [PubMed: 10650103]
3. Chen J, Stubbe J. Nat. Rev. Cancer. 2005; 5:102–112. [PubMed: 15685195]
4. Galm U, Hager MH, Van Lanen SG, Thorson JS, Shen B. Chem. Rev. 2005; 106:739–758. [PubMed: 15700963]
5. Goodwin KD, Lewis MA, Long EC, Georgiadis MM. Proc. Natl. Acad. Sci. U. S. A. 2008; 105:5052–5056. [PubMed: 18362349]
6. Buettner GR, Oberley LW. FEBS Lett. 1979; 101:333–335. [PubMed: 87348]
7. Strong JE, Crooke ST. Cancer Res. 1978; 38:3322–3326. [PubMed: 80263]
8. Lown JW, Joshua AV. Biochem.Pharmacol. 1980; 29:521–532. [PubMed: 6154464]
9. Tueni EA, Newman RA, Baker FL, Ajani JA, Fan D, Spitzer G. Cancer Res. 1989; 49:1099–1102. [PubMed: 2465080]
10. Nicaise C, Ajani J, Goudeau P, Rozencweig M, Levin B, Krakoff I. Cancer Chemother. Pharmacol. 1990; 26:221–222. [PubMed: 1694112]
11. Nicaise C, Hong WK, Dimery W, Usakewicz J, Rozencweig M, Krakoff I. Invest. New Drugs. 1990; 8:325–328. [PubMed: 1703132]
12. Du L, Sanchez C, Chen M, Edwards DJ, Shen B. Chem. Biol. 2000; 7:623–642. [PubMed: 11048953]
13. Shen B, Du L, Sanchez C, Edwards DJ, Chen M, Murrell JM. J. Nat. Prod. 2002; 65:422–431. [PubMed: 11908996]
14. Galm U, Wang L, Wendt-Pienkowski E, Yang R, Liu W, Tao M, Coughlin JM, Shen B. J. Biol. Chem. 2008; 283:28236–28245. [PubMed: 18697737]
15. Galm U, Wendt-Pienkowski E, Wang L, George NP, Oh T-J, Yi F, Tao M, Coughlin JM, Shen B. Mol. BioSyst. 2008; 5:77–90. [PubMed: 19081934]
16. Wang L, Tao M, Wendt-Pienkowski E, Galm U, Coughlin JM, Shen B. J. Biol. Chem. 2009; 284:8256–8264. [PubMed: 19189972]
17. Gust B, Challis GL, Fowler K, Kieser T, Chater KF. Proc. Natl. Acad. Sci. U. S. A. 2003; 100:1541–1546. [PubMed: 12563033]
18. Calafat A, Won H, Marzilli L. J. Am.Chem. Soc. 1997; 119:3656–3664.
19. Mirabelli CK, Huang CH, Fenwick RG, Crooke ST. Antimicrob. Agents Chemother. 1985; 27:460–467. [PubMed: 2408562]
20. Boger DL, Cai H. Angew. Chem. Int. Ed. 1999; 38:448–476.
21. Sznaidman ML, Hecht SM. Org. Lett. 2001; 3:2811–2814. [PubMed: 11529763]
22. Leitheiser CJ, Smith KL, Rishel MJ, Hashimoto S, Konishi K, Thomas CJ, Li C, McCormick MM, Hecht SM. J. Am. Chem. Soc. 2003; 125:8218–8227. [PubMed: 12837092]
23. Ma Q, Xu Z, Schroeder BR, Sun W, Wei F, Hashimoto S, Konishi K, Leitheiser CJ, Hecht SM. J. Am. Chem. Soc. 2007; 129:12439–12452. [PubMed: 17887752]

24. Chapuis JC, Schmaltz RM, Tsosie KS, Belohlavek M, Hecht SM. J. Am. Chem. Soc. 2009; 131:2438–2439. [PubMed: 19187019]
25. Du L, Shen B. Chem. Biol. 1999; 6:507–517. [PubMed: 10421758]
26. Du L, Chen M, Sanchez C, Shen B. FEMS Microbiol. Lett. 2000; 189:171–175. [PubMed: 10930733]
27. Sanchez C, Du L, Edwards DJ, Toney MD, Shen B. Chem. Biol. 2001; 8:725–738. [PubMed: 11451672]
28. Schneider TL, Shen B, Walsh CT. Biochemistry. 2003; 42:9722–9730. [PubMed: 12911314]
29. Du L, Chen M, Zhang Y, Shen B. Biochemistry. 2003; 42:9731–9740. [PubMed: 12911315]
30. Spiteller P, Bai L, Shang G, Carroll BJ, Yu TW, Floss HG. J. Am. Chem. Soc. 2003; 125:14236–14237. [PubMed: 14624546]
31. Kulathila R, Merkler KA, Merkler DJ. Nat. Prod. Rep. 1999; 16:145–154. [PubMed: 10331284]
32. Sambrook, J.; Russell, DW. Molecular Cloning: a Laboratory Manual. 3rd Ed.. New York: Cold Spring Harbor Laboratory Press; 2001.
33. MacNeil DJ, Gewain KM, Ruby CL, Dezeny G, Gibbons PH, MacNeil T. Gene. 1992; 111:61–68. [PubMed: 1547955]
34. Kieser, T.; Bibb, MJ.; Buttner, MJ.; Chater, KF.; Hopwood, DA. Practical Streptomyces Genetics. 2nd Ed.. Norwich, UK: John Innes Foundation; 2000.
35. Parekh S, Vinci VA, Strobel RJ. Appl. Microbiol. Biotechnol. 2000; 54:287–301. [PubMed: 11030563]
36. Liang J, Xu Z, Lin J, Cen P. Enzyme Microb. Technol. 2008; 42:145–150.

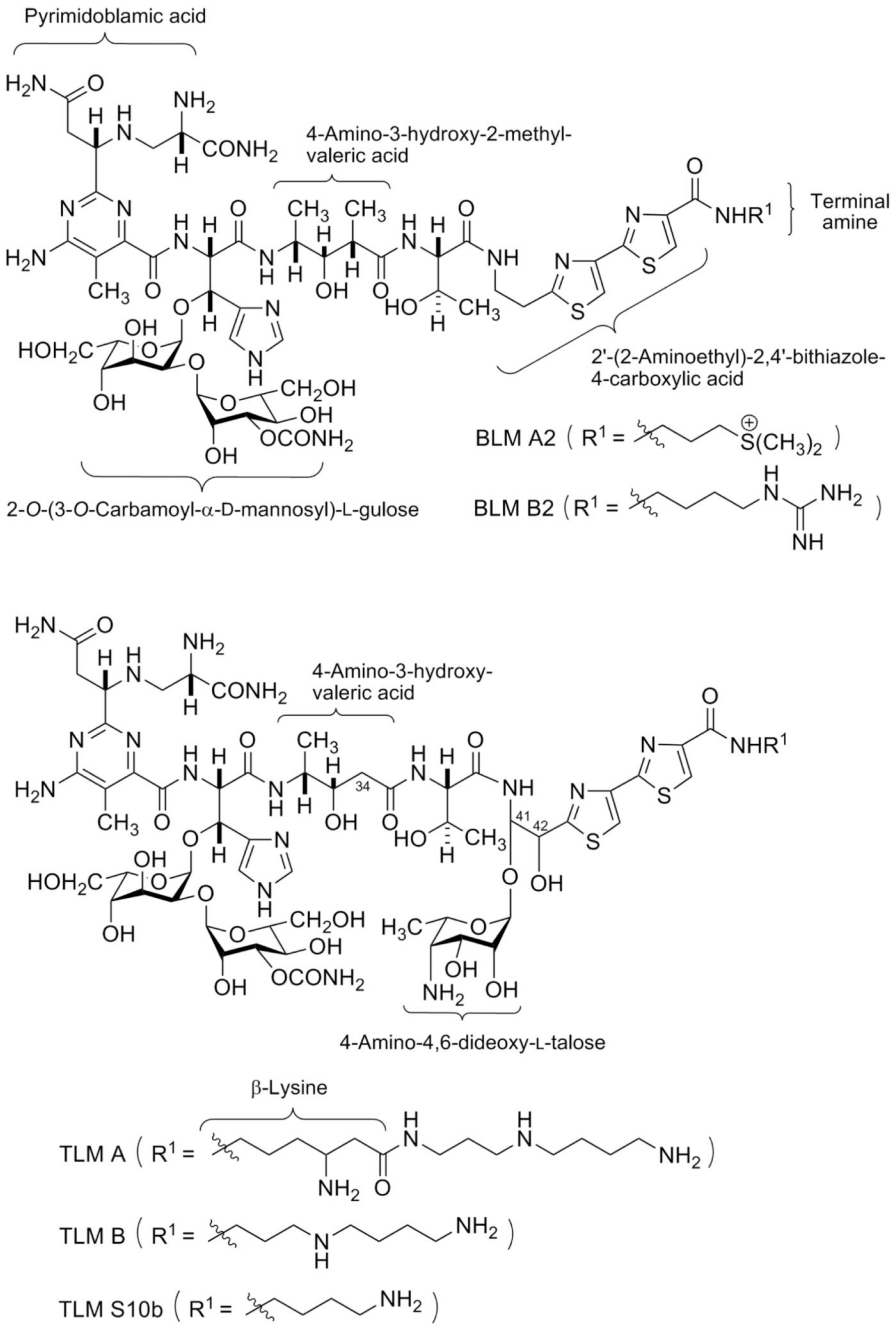

Fig. 1.

Structures of selected members of the bleomycin family of antitumor antibiotics BLM A2, BLM B2, TLM A, TLM B, and TLM S10b.

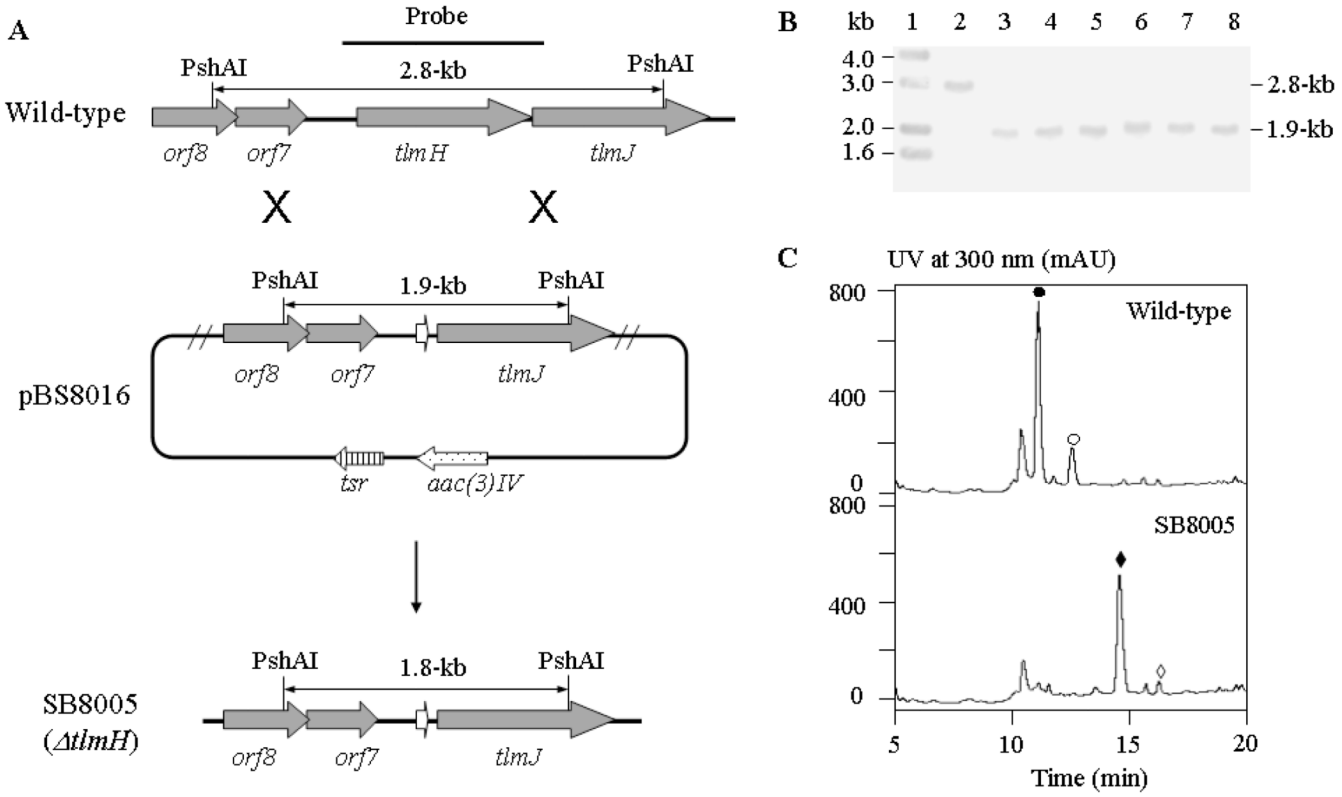

Fig. 2.

Inactivation of *tlmH* by in-frame deletion in *S. hindustanus*. (A) Construction of the *ΔtlmH* mutant SB8005 strain and restriction map of the *S. hindustanus* wild-type and SB8005 strains showing fragment sizes upon *Psh*AI digestion. (B) Southern analysis of the *ΔtlmH* mutant (lanes 3–8, six SB8005 isolates) and *S. hindustanus* wild-type (lane 2) genomic DNA digested with *Psh*AI using a 1.6-kb PCR-amplified fragment as a probe. Lane 1, molecular weight marker. (C) HPLC analysis of TLM production in the *S. hindustanus* wild-type and the *ΔtlmH* mutant SB8005 strains. Symbols: ●, TLM A; ○, TLM B; ♦, TLM H-1; ◊, TLM H-2.

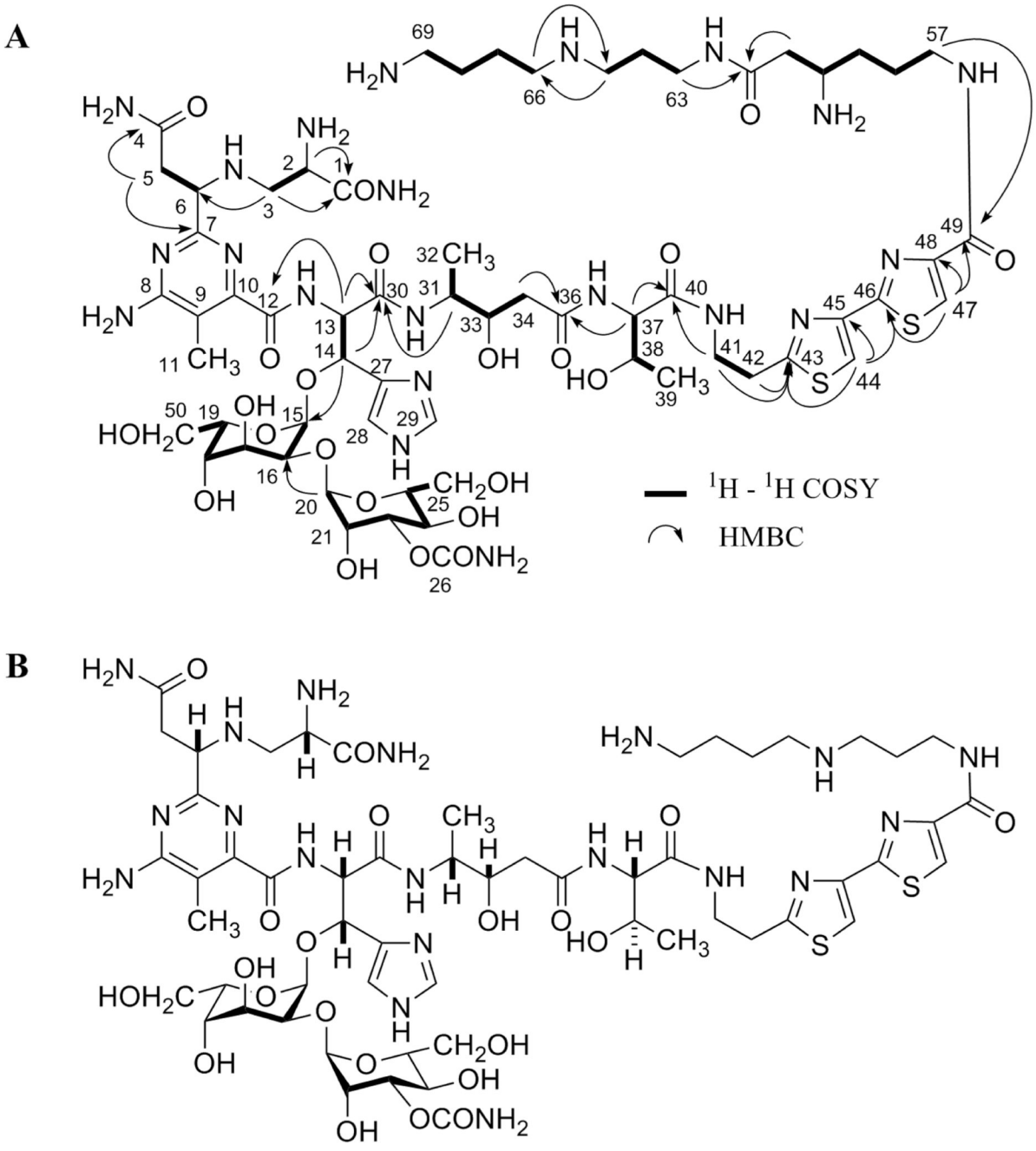

Fig. 3.

The structures of (A) TLM H-1 supported by key ^{1}H - ^{1}H COSY and HMBC correlations and (B) TLM H-2 deduced on the basis of LC-ESI-MS analysis.

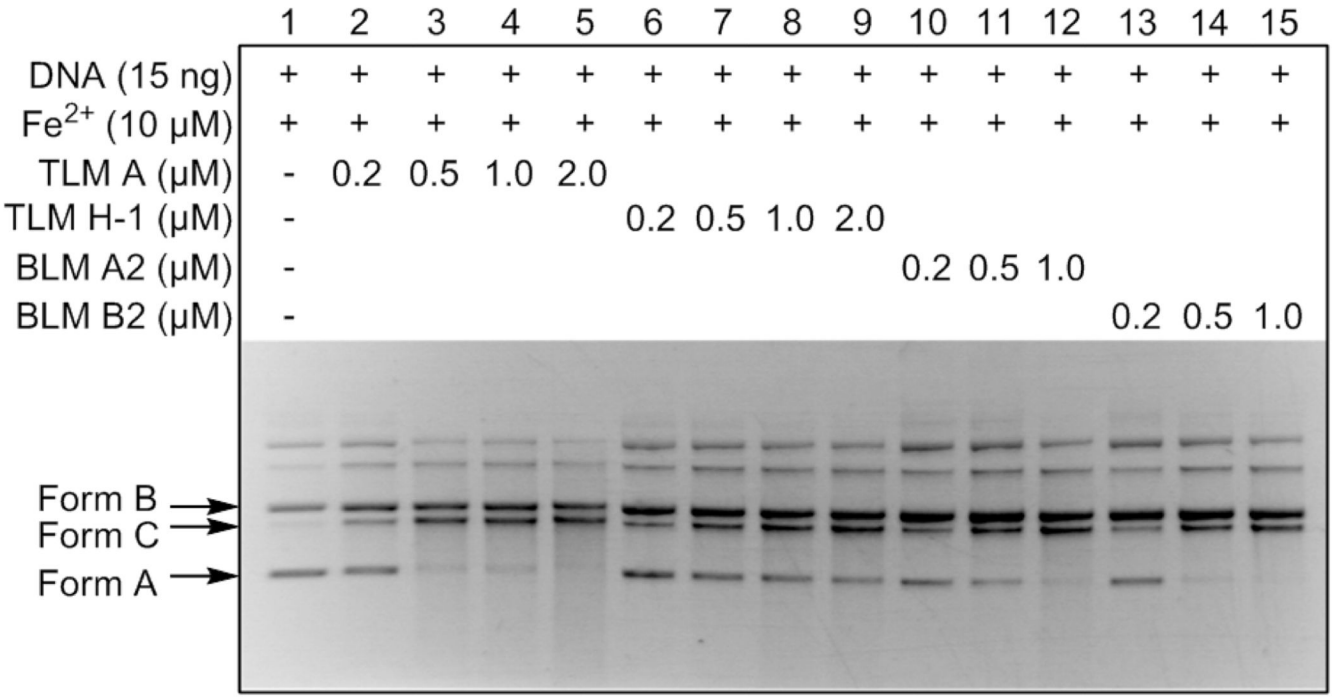

Fig. 4.

DNA cleavage activities of TLM H-1 in comparison with TLM A, BLM A2, and BLM B2 as observed in plasmid relaxation and linearization assays with pBluescript II SK(+). Form A, supercoiled plasmid DNA; form B, open-circular plasmid DNA; form C, linearized plasmid DNA.

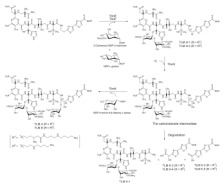

Fig. 5.
The revised pathway for TLM biosynthesis featuring TlmH-catalyzed hydroxylation of both C41 and C42 to afford labile carbinolamide intermediates and TlmK-catalyzed subsequent glycosylation of their hemiaminal hydroxyl groups as the final two steps.

Table 1

^{13}C NMR and ^{1}H NMR data of TLM H-1 [D_2O, 3-trimethylsilyl[2,2,3,3,-$^{2}H_4$]propionate, δ (ppm) (*J* = HZ)][a]

No.	δ_C	δ_H	No.	δ_C	δ_H
1	174.7		32	17.3	1.18 d (7.0)
2	55.4	4.01 m[b]	33	73.6	4.05 m[b]
3	50.1	3.40 dd (14.0,6.5), 3.50 m[b]	34	42.5	2.44 dd (15.0,3.0), 2.50 dd (15.0, 9.5)
4	178.9		36	176.9	
5	43.0	2.91dd (16.0,7.5) 2.95 m[b]	37	62.1	4.20 d (4.5)
6	62.5	4.50 dd (12.5,7.0)	38	69.8	4.19 m[b]
7	168.2		39	21.7	1.10 d (6.9)
8	167.2		40	175.0[b]	
9	114.5		41	41.8	3.30 m[b]
10	155.7		42	34.8	3.65 m[b]
11	13.4	1.97 s	43	173.4	
12	170.4		44	121.9	8.21 s
13	59.5	5.14 d (8.0)	45	149.7	
14	76.5	5.43 d (8.0)	46	165.5	
15	100.8	5.30 d (3.5)	47	127.7	8.09 s
16	69.6	4.07 m[b]	48	151.8	
17	71.8	3.95 m[b]	49	165.9	
18	70.9	3.98 m[b]	50	62.8	3.40 m[b], 3.51 m[b]
19	73.3	4.12 m[b]	57	41.6[b]	3.49 m
20	101.3	5.05 brs	58	27.4	1.76 br[b]
21	71.2	4.18 m[b]	59	32.3	1.76 br[b]
22	77.2	4.80 m[b]	60	51.4	3.65 m[b]
23	67.7	3.86 m[b]	61	39.6	2.62 dd (16.0,5.0), 2.71 dd (16.0,10.0)
24	76.2	3.86 m[b]	62	175.0[b]	
25	63.8	3.80 m[b], 3.95 m[b]	63	39.0	3.26 m

No.	δ_C	δ_H	No.	δ_C	δ_H
26	160.9		64	28.3	1.88 m
27	137.7		65	48.0	3.05 m[b]
28	120.7	7.65 s	66	49.8	3.05 m[b]
29	139.7	8.83 s	67	25.6	1.76 br[b]
30	172.5		68	26.8	1.76 br[b]
31	52.6	4.05 m[b]	69	41.6[b]	3.05 m[b]

[a] Assignment confirmed by ^{1}H-^{1}H correlation spectroscopy; total correlation spectroscopy; heteronuclear single quantum coherence; and heteronuclear multiple bond correlation spectra obtained at 500 MHz and 125 MHz.

[b] Overlapped signal.